HYDROMECHANICAL MODELLING OF FRACTURED ROCK MASSES
USING COUPLED NUMERICAL SCHEMES

Derek Elsworth* and Richard E. Goodman**

*The Pennsylvania State University, University Park, PA 16802
**University of California, Berkeley, CA 94720

ABSTRACT

Coupled boundary element-finite element
procedures are presented for the hydraulic
analysis of discretely fractured rock masses.
The respective analyses evaluate flow in three
dimensional, rigid fractured media in the time
domain and two dimensional porous-fractured
deformable media. For flow analysis, a direct
boundary element procedure is invoked to yield
the elemental geometric conductance of an
individual fissure disc with reduced degrees of
freedom. The global matrices are cast in finite
element format and extended to the transient
domain. Coupled analysis for deformation
utilizes an indirect displacement discontinuity
formulation to represent the behavior of the
fractured elastic continuum. Flow within both
fissures and blocks is achieved using a revised
boundary element-finite element procedure. The
numerical formulations are illustrated, in all
cases, to provide a tractable and computationally
efficient means of handling spatially large
systems of fractures in either two or three
dimensional space. Illustrative examples are
included to emphasise the capabilities of the
methods presented.

INTRODUCTION

The safe immobilisation of radioactive waste
in geologic formations requires that predictive
techniques and analyses must be capable of
extending to time spans of the order of tens of
hundreds of years. The most favored host rocks
for a repository comprise low permeability
formations about which little field and design
data are presently available. The very nature of
these low permeability and sparsely fractured
rock formations negates the application of well
tested homogenisation techniques in attempting
correlations with "equivalent" continua. This
observation is equally valid with regard to both
uncoupled flow characterisation and with respect
to coupled rock mass deformations. The discrete
nature of fracturing within the masses require
that revised numerical formulations are available
that are capable of efficiently evaluating both
uncoupled and coupled flow-deformation behavior.

Consideration within the following will be
limited to evaluation of the response of sparsely
fractured masses. Representative elemental
volume considerations require that, at a certain
scale, individual fissures must be modelled
discretely (Long, 1983). The large number of
fissures comprising a typical section of the rock
mass requires that numerical models appropriate
to the problem geometry reflect the utmost in
computational efficiency. This is necessary if
the capacity of currently available hardware is
not to be exceeded for even relatively modest
realizations of fissure density. Fractured rock
masses are genuinely three dimensional with a
compatible two dimensional idealisation being
difficult to either determine or justify. This
situation is further compounded on realizing that
any two dimensional analogy of a three
dimensional system will always underestimate
potential hydraulic conductivity. Two
dimensional analyses will, therefore, be expected
to err on the unsafe side for the specific task
of waste immobilisation predictions.

While discrete modelling of individual rock
fissures may be desirable in the near field, the
domain external boundaries must also be
appropriately represented. For the effective
infinite or semi-infinite extent of the mass
surrounding a repository, arbitrary truncation of
the discretised domain may result in incorrect
evaluation of fluid flow or mass displacement
fields. It is important that these external
boundaries are correctly represented as the
radius of influence increases with elapsed time.

For modelling of flow in sparsely fractured
rock masses it is convenient if domain
discretisation is restricted purely to individual
fractures. Boundary element techniques may be
invoked, based on a restricted discretisation, to
evaluate linear flow and linear elastic
deformation of the surrounding body.
Nonlinearities with regard to flow turbulence
within and inelastic stress-displacement across
the individual fissures may be adequately
accommodated. For likely repository scenarios,
flow turbulence is not considered a major concern
although nonlinear rock joint response may be
shown to be an important factor.

STEADY ANALYSIS

For an array of randomly distributed fissure
discs in three dimensional space, a single
fissure disc may be isolated as the basic
geometric conduit. An array of three discs is
illustrated in Figure 1. The central disc is
isolated with appropriate hydraulic connections
in two dimensional space in Figure 2. The direct
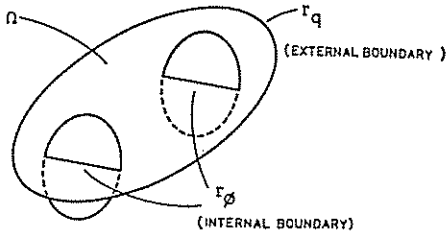boundary constraint equation for steady linear

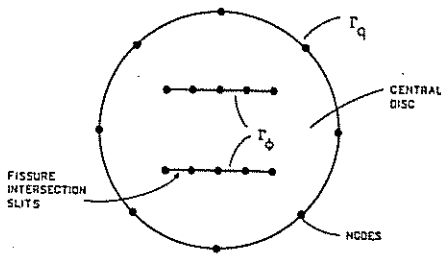Figure 1. Perspective view of three intersecting fissure discs.

Figure 2. Boundary element representation of the central disc of Figure 1.

potential flow may be stated as (Jawson, 1977; Bannerjee, 1980)

$$c(p)\phi(p) + \int_\Gamma V(p,q)\phi(q)\ d\Gamma = \int_\Gamma \Phi(p,q)v(q)\cdot\bar{n}\ d\Gamma$$

$$\ldots (1)$$

where $V(p,q)$, $\Phi(p,q)$ are kernels describing, respectively, induced velocity and total hydraulic potential at point q due to a unit source at point p. The parameters of boundary potential (ϕ) and normal to the boundary velocity ($v\cdot\bar{n}$) are either supplied as boundary conditions or solved for as unknowns. All integrations are evaluated over the surface of the body (Γ) which, for the case of a two dimensional disc, comprises a line segment of closed contour. Intersections within the disc interior may be accommodated where integrations are evaluated taking due account of the free term $c(p)$. Where the source point is present on the smooth boundary, the free term is equal to $\tfrac{1}{2}\ \delta pq$ where δ is the Kroncker delta. For internal elements, the free term is equal to unity.

The integrals of equation (1) may be evaluated either in closed form or numerically. For the isoparametric representation of fissure edge contour and singularity distribution used in this work, numerical integration is necessary. A typical three noded curved element is illustrated in Figure 3. Consistent with the representation of geometry, quadratic basis functions are used in the evaluation of integrals to yield the boundary constraint equation in matrix form as

$$\underset{nxn}{\Phi}\ \underset{nx1}{v} = \underset{nxn}{V}\ \underset{nx1}{\phi} \qquad (2)$$

where Φ and V are fully populated tensors of integrated kernel functions for potential and velocity, respectively, and v and ϕ are the nodal values of normal velocity and total hydraulic potential. A total of n nodes comprise the external domain boundary. In a well posed problem either boundary nodal velocity or boundary head will be prescribed and equation (2) may be rearranged to solve for the unknowns at respective nodes. For the case of the fissure disc the external normal boundary velocity is zero although no prescribed conditions are set at the internal nodes. Symbolic rearrangement of equation (2) yields (Zienkiewicz, 1977b)

$$\underset{\sim}{v} = [\underset{\sim}{\Phi}^{-1}\ \underset{\sim}{V}]\ \underset{\sim}{\phi} \qquad (3)$$

which, for the case of m internal nodes, is equivalent to solving n + m simultaneous equations for m load cases. The resulting matrix is m x m in dimension and bears a basic facsimile to finite element format being symmetric and positive definite. Thus

$$\underset{\sim}{q} = \underset{\sim}{f}\ [\underset{\sim}{\Phi}^{-1}\ \underset{\sim}{V}]\ \underset{\sim}{\phi}\quad \equiv \underset{\sim}{q} = \underset{\sim}{k}\ \underset{\sim}{\phi} \qquad (4)$$

where q is a vector of nodal discharges and f is a vector of integrated basis functions relating nodal velocities to discharge. In the condensation procedure the external edge degrees of freedom are redundant and the internal degrees of freedom may be reduced to a minimum of one per intersection. Global assembly may be completed in standard finite element fashion to yield a reduced degree of freedom system.
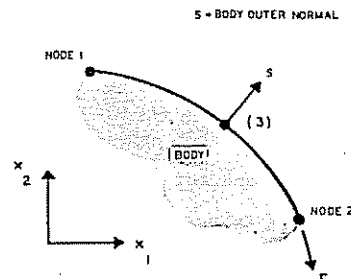

Figure 3. Isoparametric form of a single three-noded line element.

APPLICATION

To emphasize the potential of the proposed formulation, consider the network illustrated in Figure 4(a). The system comprises a total of six circular fissure discs and a single vertical square fissure. All circular disc sets are arranged with equal separation in their respective orientations. The single rectangular disc intersects all circular fissure discs and provides hydraulic connection between them in addition to the horizontal trace intersections between the circular discs. The discretised forms of two typical discs are illustrated in Figure 4(b), the full network comprising 57 nodal degrees of freedom. Although it is possible to further condense the system degrees of freedom, accurate mapping of potential gradient within the system requires that sensible nodal density be retained.

For the 57 node system it is possible to rapidly analyse a number of different hydraulic scenarios for contrasting relative conductivities of the discs. The parallel plate analogy in any convenient linear form may be used to obtain suitable values for disc hydraulic conductivity from fissure aperture and roughness. Nodal meshing input data preparation is not excessive. Matrix reduction to obtain the reduced degree of freedom system took 50 CPU seconds on a DEC Vax 11/780. This step has only to be completed once, the tensors for increased fissure conductivity being scalar multiples of the original disc tensors. Global matrix assembly and LU factorization took 13 CPU seconds with an additional 3 CPU seconds required per additional execution case.

The results for sample runs on the fissure geometry illustrated in Figure 4(a) are illustrated in Figure 5. A unit drop in hydraulic potential is applied between the intersection traces identified in Figure 4(a). Transmissivities (K_h, K_v) for the circular discs are arranged for two comparative cases as both isotropic (K_h, K_v = 1.0) and horizontally dominant ($K_h/K_v \approx 100.0$). The transmissivity of the backing square fissure is varied throughout.

Under the unit head differential, the importance of accommodating the truly three dimensional nature of the fissure geometry is illustrated. The baseline characteristics for the hydraulic behavior of both a two-dimensional lattice and the vertical square fissure are illustrated. Where the square fissure provides poor hydraulic connectivity ($K_z/K_y < 0.1$) the assemblage behaves in an essentially two-dimensional manner. As the hydraulic conductivity of the backing disc is increased, the performance of the system is dominated by this major structural feature. Lack of account for the influence of this feature in evaluating the hydraulic response of the medium would clearly be inappropriate. The errors that this neglect may entrain into the analysis could clearly overshadow the applicability of a more complex two dimensional analysis accounting for the hydromechanical behavior of rock fissures. An important consideration in selection of an
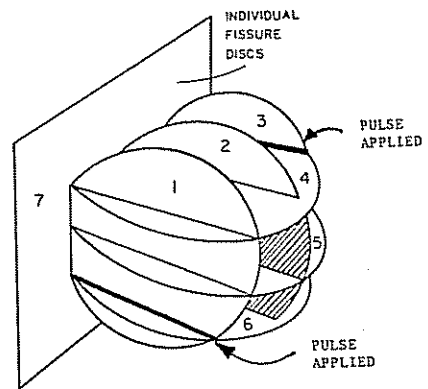

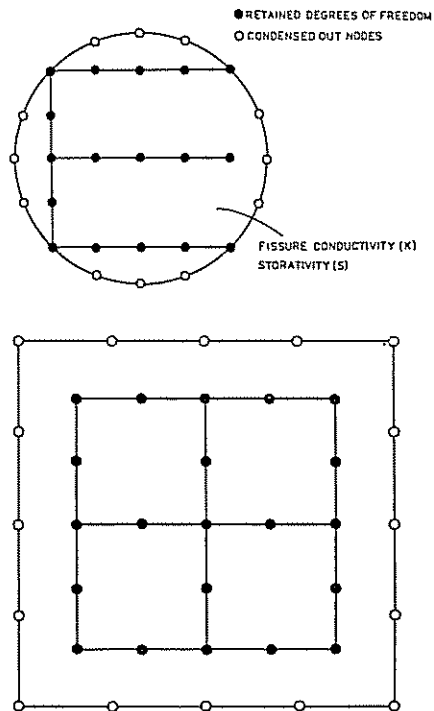Figure 4(a). Perspective view of seven disc assemblage.

Figure 4(b). Representative constituent discs.

appropriate level of modelling "sophistication" might therefore include spatial dimentionality of the analysis.

TRANSIENT ANALYSIS

In finite element form, the transient response of a system at any moment in time (t) may be represented by the matrix identity.

$$\underline{K}\ \underline{\phi}_t + \underline{S}\ \underline{\dot{\phi}}_t = \underline{q}_t \qquad (5)$$

where $\underline{\phi}_t$ and $\underline{\dot{\phi}}_t$ are respectively vectors of total head and time derivative of head. Prescribed nodal discharges (q_t) are known boundary conditions and $\underline{K}$ and $\underline{S}$ are tensors of geometric conductance and storativity. Stability
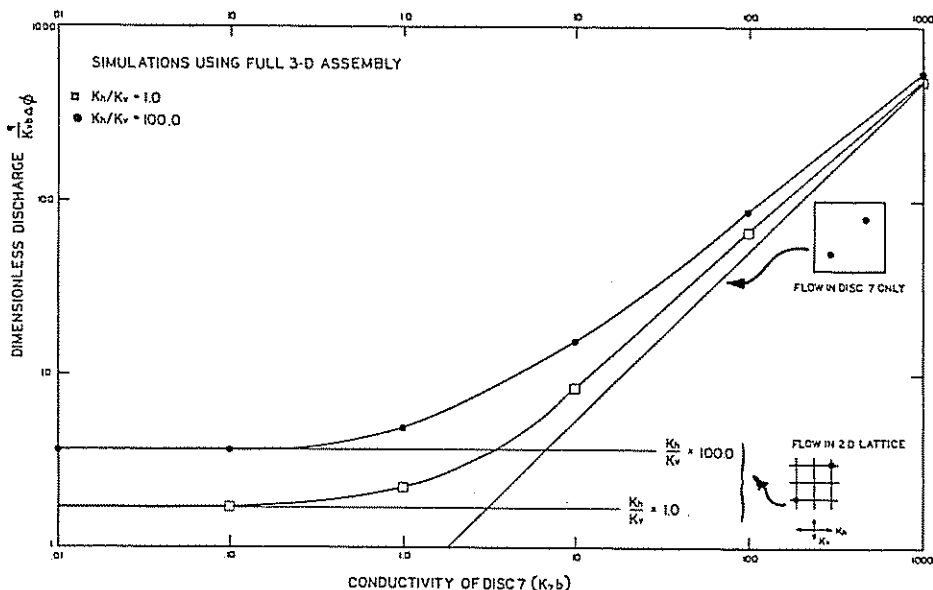
Figure 5. Variation in steady discharge through the fissure assemblage with varied component conductivities.

considerations dictate that a lumped vector of storativity terms (Newman, 1977) is used whereby equation (5) may be rearranged to yield

$$\underline{K}^* \ \underline{\phi}_{t+\Delta t} = \underline{q}^*_{t+\Delta t} \tag{6}$$

where

$$\underline{K}^* = (\underline{K} + \underline{S}/\Delta t) \tag{7}$$

$$\underline{q}^*_{t+\Delta t} = q_{t+\Delta t} + \underline{\phi}_t \ \underline{S}/\Delta t \tag{8}$$

Linear variation in nodal head within a single time step is assumed, the integration scheme being unconditionally stable for any time increment Δt (Polivka, 1976).

The sum of entries within the elemental storativity vector must equal the total domain storativity. For closed contour problems, such as the fissure disc application, the total storativity for the domain is the product of area integral, mean fissure aperture and specific storage. This total must then be distributed between nodes in any acceptable fashion. Nodal weighting of the storativity terms may be achieved using finite element basis functions if elements are meshed throughout the disc (Zienkiewicz, 1977a). This would, however, be counterproductive in that development of the solution procedure is motivated by the ease with which element meshing may be achieved. Any tributary area distribution technique may be adopted. It has been found satisfactory to distribute the total storativity between nodes based on the magnitude of the diagonal terms of the elemental geometric conductivity matrix, $\underline{K}$ (Elsworth, 1985). Since the nodal weightings used in finite element analysis are somewhat arbitrary, the consequences of the chosen

distribution procedure are minimised providing large numbers of discs comprise a complete network.

The matrix identity in equation (6) requires that the $\underline{K}^*$ matrix is factored only once. The variable form of the prescribed discharge vector ($\underline{q}^*$) represents successive loading cases for which backsubstitition yields the time-updated magnitudes of nodal potentials ($\underline{\phi}_{t+\Delta t}$).

APPLICATION

For the model network illustrated in Figure 4(a), the transient performance is gauged using this compacted scheme. The execution times quoted in the previous section for steady flow are representative for the transient condition with solution for a single additional load case being equivalent to integrating forward a single time step. The time marching scheme has been shown capable of representing the transient performance of a single disc with only one degree of freedom retained per intersection (Elsworth, 1985). For the model geometry of Figure 4(a), a distinct advantage is obtained in accurately mapping changes in domain potential if multiple nodes are retained. The reduced system is retained at 57 nodes with a unit pulse applied at the basal intersection (Figure 4(a)) and all other outlets sealed.

Transient response curves for the sealed domain are shown in Figures 6 and 7 for the variety of mixed conductivity conditions of the steady analyses. The transient hydraulic response of the system for homogeneous conductivity in the six circular discs is shown in Figure 6. Curves A through C are respectively for the behavior of the lattice only, the square disc only and the combined lattice and square disc. The highest initial time history of
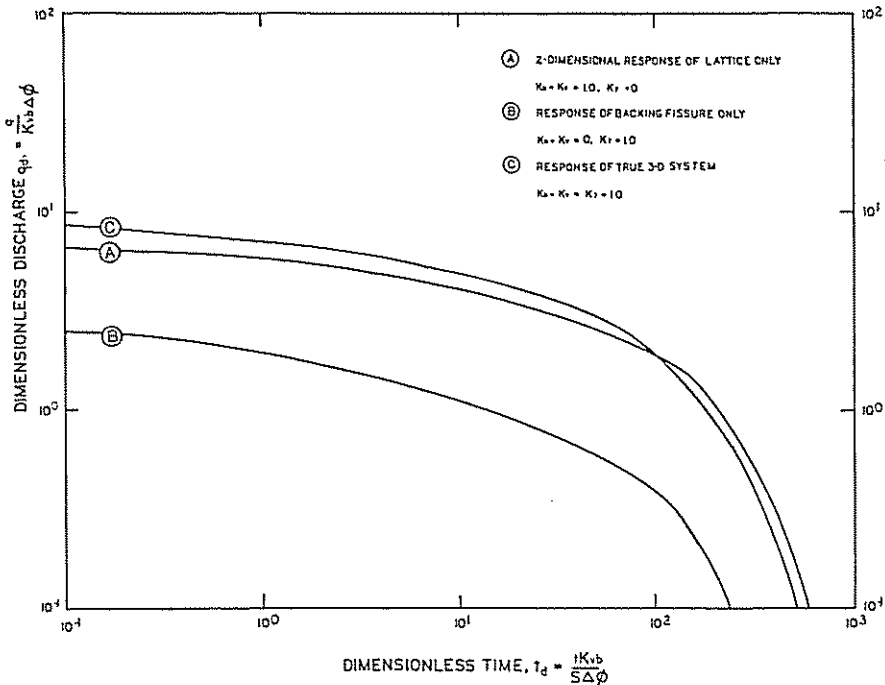
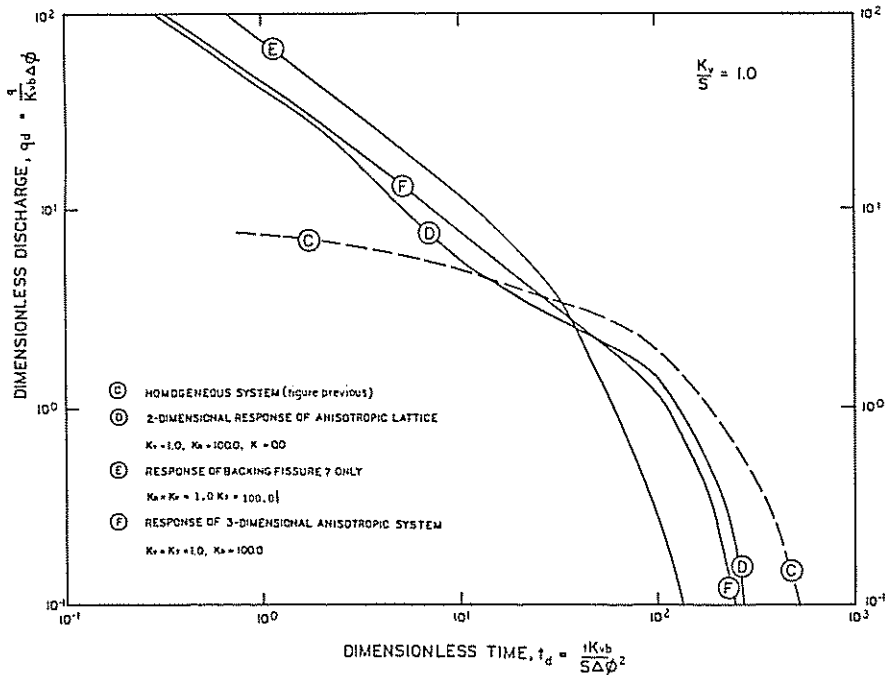Figure 6. System transient response for two and three dimensional analyses.

Figure 7. System transient response for anisotropic domain analyses.

discharge is for the combined system with the next highest being for the two dimensional lattice alone. This behavior might be expected if it is noted that discharge from the crossed lattice is along a specific length. The lowest of the discharge histories is for the single square disc alone. The sluggish response of the system at early dimensionless times ($t_d < 1.0$) is a facet of the numerical analysis. The initial perturbation gradient within the disc system is controlled, to great extent, by the nodal spacing within discs. Hence, the early time performance is strongly controlled by this factor.

The response scenarios are investigated for non uniform conductivity within discs in Figure 7. Curves D through F represent the behavior of the system with; (D) high conductivity of the horizontal discs ($K_h/K_v = 100$, $K_7/K_v = 0.0$) with no backing square fissure, (E) uniform conductivity of the lattice with the backing disc of much higher conductivity ($K_h/K_v = 1.0$, $K_7/K_v = 100.0$), and (F) high conductivity of the horizontal discs with the backing fissure of unit conductivity ($K_h/K_v = 100$, $K_7/K_v = 1.0$). The presence of a highly conductive backing fissure is shown to accelerate drainage and ultimate depletion of the system. A similar effect is

evident where high horizontal conductivity is apparent. With no backing fissure, the system response exhibits a definite discontinuity at dimensionless time of $t_d = 10$. This represents full drainage of the horizontal fissures with the low conductivity vertical system beginning to contribute to the supply. This discontinuity in behavior is masked where the backing fissure is present to aid discharge.

For curves D through F of Figure 7 the spurious numerical response in the initial drainage period (small t_d) is not evident. This factor is as a result of the high conductivity of single network components giving a lateral shift to these data. The restriction of accurate modelling at small dimensionless times is not considered a serious detraction from the practical applicability of an otherwise promising technique. If the response of a large volume of rock mass is required then, by definition, the finite transit velocity of the perturbation pulse infers that the late behavior is of most significance. The generality of formulation further allows increased meshing density in regions where transient gradients are likely to be excessive. Refinements of this nature are only relevant if viewed relative to the quality of geologic data available.

COUPLED FLOW-DETERMINATION ANALYSIS

Emphasis within the previous has been to illustrate the applicability of boundary element formulations in reducing system degrees of freedom to a minimum. Where the analysis is extended into the realm of rock mass deformation this basic premise may be adhered to if the nonlinear rock fissure deformation response is restricted only to the discontinuity traces in two dimensions.

Of the available point force and point displacement formulations available the displacement discontinuity method is most applicable. The basic kernel function is a point discontinuity in displacement from which the induced stresses and displacements in the surrounding medium may be determined (Wiles, 1982). The method is particularly suited to analysis of fissured media in that the point shear and normal singularities represent the physical properties of shear displacement and aperture change across individual joints. The basic matrix identity for two dimensional analysis is (Crouch, 1976)

$$\begin{bmatrix} \sigma_n \\ \tau \end{bmatrix} = \begin{bmatrix} A_{nn} & A_{ns} \\ A_{sn} & A_{ss} \end{bmatrix} \begin{bmatrix} D_n \\ D_s \end{bmatrix} \quad (9)$$

where σ_n, τ are total normal and shear stresses induced in the medium by unit nodal normal and shear displacement discontinuities D_n, D_s. The linking $\underline{A}$ matrix contains the appropriate integrals of kernel functions. Appropriate magnitude of the stress vector terms may be obtained from the known field stresses and required boundary conditions. Where linear joint

stiffness in closing is accommodated a further solution constraint is added such that

$$\begin{bmatrix} \sigma_n \\ \tau \end{bmatrix} = \begin{bmatrix} K_n & 0 \\ 0 & K_s \end{bmatrix} \begin{bmatrix} D_n \\ D_s \end{bmatrix} \quad (10)$$

where K_n, K_s are the linear fissure stiffnesses under normal and shear loading. Solution of (9) subject to (10) yields a distribution of fissure apertures for which the flow field may be evaluated. Linearly varying displacement discontinuities and linearly tapering fissure finite elements are used in the analyses presented. Previous analysis using constant displacement discontinuities and constant fissure flow elements within impermeable wall rock has been reported (Cruikshank, 1979).

For two dimensional analysis an example porous flow domain containing a single, centrally discharging fracture is illustrated in Figure 8. The formation hydraulic conductivity (K_m) is set to unity. A unit head differential is set between the producing wellbore at the fissure centre and the outer boundary at radius 50 meters. The porous domain is represented exclusively by boundary elements. Dipole flow elements are meshed on the internal fracture extent to which linearly tapering line flow elements are connected. Linear displacement discontinuity elements are meshed along the fracture length.
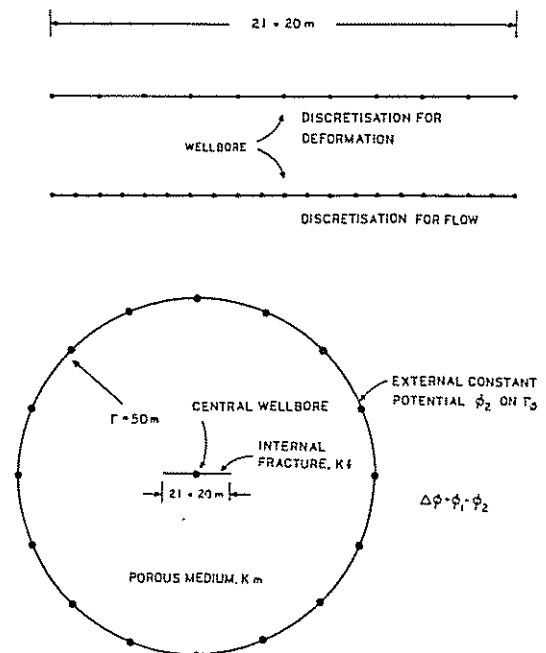

Figure 8. Discretisation for deforming fracture flow. Central fissure discretisation above.

For uncoupled solution, the variation in potential head with length along the fissure is illustrated for different apertures and hence conductivity in Figure 9. For an impermeable fissure ($K_f = 0$), the head variation corresponds to radial, porous media flow. For increased conductivity of the fissure, the flow patterns are increasingly dominated by the presence of the conduit. Where the equivalent fissure conductivity exceeds formation conductivity by a factor of 10^4, the fracture acts as a conduit of infinite conductivity.
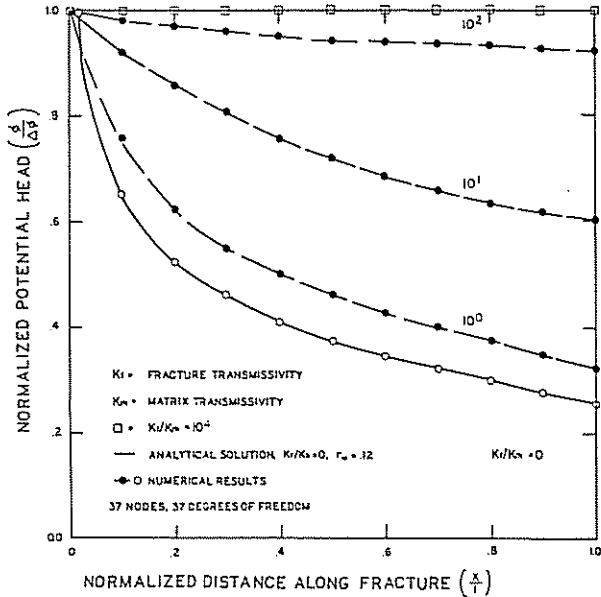

Figure 9.   Variation in potential along the fracture of Figure 8, for different fracture conductivities.

The effect of including rock mass deformability within the analysis is illustrated for the single fissure geometry in Figure 10. For fluid injection, hydraulic opening of the fissure is illustrated to have a profound effect on the head distribution along the feature. The aperture distribution in opening is controlled by the elastic parameters of the intact rock. The resistance to opening under a prescribed increase in fluid pressure is increased with increased stiffness of the surrounding mass. All solutions were completed retaining 37 flow and 22 displacement degrees of freedom. Coupled solutions were completed in under 60 seconds CPU time on a DEC Vax 11/780.

DISCUSSION AND CONCLUSIONS

A variety of coupled models are presented that are capable of efficiently analysing two and three dimensional flow problems in porous and fractured media. Coupling of boundary element and finite element procedures are shown to provide optimisation in solution efficiency where the innate advantages of each formulation are emphasised. Consistent use of appropriate element basis functions provides compatibility between all formulations presented and the
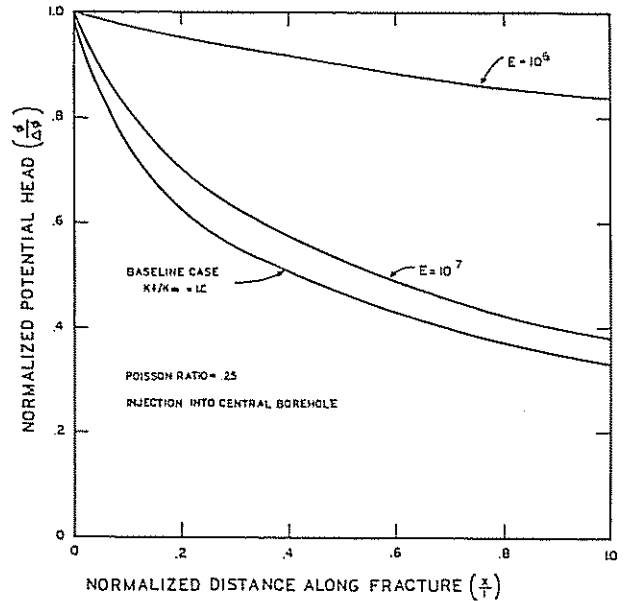

Figure 10.   Variation in normalised potential along the fracture of Figure 8 for coupled hydromechanical analysis.

coupled flow deformation analyses. Ease of data input and minimised global equation size is maintained using the boundary element procedures. The displacement discontinuity matrices are in all cases fully populated. Where coupled procedures are used to condense the elemental conductivity matrices for individual fissure discs, the resulting matrices are, in all cases, positive definite, symmetric and sparsely populated. The reduction procedure retains computations at an elemental or disc level prior to global matrix assembly. As such, the procedure is ideally suited to mini or micro-computer implementation.

Considerable insight into the projected hydromechanical behavior of rock masses may be afforded by coupled numerical models. Coupled numerical schemes offer strong computational advantages over more generally used methods. The complexity of rock masses and truly three dimensional extent of the structural features dictate that truly three dimensional models should be employed. Extension into the third dimension requires that maximum coding and formulation efficiency is maintained. Coupled finite element-boundary element procedures have the potential to achieve this goal.

The example results for three dimensional analysis in a rigid fractured rock mass illustrate the importance of considering out of plane features. Both steady discharge and the transient response are influenced by a major throughgoing feature. Behavior is truly three dimensional and does not readily conform to a two dimensional analogue. The errors that may be entrained by not considering the true extent of the structural features may possibly outweigh the advantages of completing coupled analyses in two

dimensions. Judicious use of all available
techniques is clearly desirable to aid successful
location and commissioning of a terminal waste
facility.

ACKNOWLEDGEMENTS

REFERENCES

Bannerjee, P. K. and Butterfield, R. (1981)
"Boundary Element Methods in Engineering
Science," McGraw-Hill (U.K.).

Crouch, S. L. (1976) "Analysis of Stresses and
Displacements Around Underground Excavations: An
Application of the Displacement Discontinuity
Method," RANN Program, National Science
Foundation.

Cruickshank, D. J. and Curran, J. H. (1979)
"A B.I.E. Approach to Modelling Fluid Flow in
Discontinuous Rock Masses," Proceedings of the
Seventh Canadian Congress of Applied Mechanics,
Sherbrooke, 887-888.

Elsworth, D. (1985) "The Transient Hydraulic
Response of Three Dimensional Sparsely Fractured
Rock Masses," University of Toronto, Department
of Civil Engineering, Internal Report.

Jawson, M. A. and Sym, G. T. (1977) "Integral
Equation Methods in Potential Theory and
Elastostatics," Academic Press.

Long, J. C. S. (1983) "Investigation of
Equivalent Porous Medium Permeability in Networks
of Discontinuous Fractures," Ph.D. Thesis,
University of California, Berkeley.

Neuman, S. P. and Narasimhan, T. N. (1977) "Mixed
Explicit-Implicit Iterative Finite Element Scheme
for Diffusion Type Problems: I. Theory," Int.
Journ. for Num. Meth. in Eng., VII, 309-323.

Polivka, R. M. and Wilson, E. L. (1976), "Finite
Element Analysis of Nonlinear Heat Transfer
Problems," Department of Civil Engineering,
University of California, Berkeley, UCSESM 76-2.

Wiles, T. D. and Curran, J. H. (1982) "A General
3-D Displacement Discontinuity Method," Proc. 4th
Int. Conference on Numerical Methods in
Geomechanics, Edmonton, 103-111.

Zienkiewicz, O. C. (1977) "The Finite Element
Method," Third Edition, McGraw-Hill (U.K.).

Zienkiewicz, O. C., Kelly, D. W. and Bettes, P.
(1977), "The Coupling of the Finite Element
Method and Boundary Element Procedures," Int. J.
for Num. Meth. in Eng., VII, 355-375.